Structural Basis for Phosphotyrosine Peptide Recognition by Protein Tyrosine Phosphatase 1B

Zongchao Jia, David Barford,* Andrew J. Flint, Nicholas K. Tonks

The crystal structures of a cysteine-215 → serine mutant of protein tyrosine phosphatase 1B complexed with high-affinity peptide substrates corresponding to an autophosphorylation site of the epidermal growth factor receptor were determined. Peptide binding to the protein phosphatase was accompanied by a conformational change of a surface loop that created a phosphotyrosine recognition pocket and induced a catalytically competent form of the enzyme. The phosphotyrosine side chain is buried within the protein and anchors the peptide substrate to its binding site. Hydrogen bonds between peptide main-chain atoms and the protein contribute to binding affinity, and specific interactions of acidic residues of the peptide with basic residues on the surface of the enzyme confer sequence specificity.

The dephosphorylation of phosphotyrosine (pTyr) residues by protein tyrosine phosphatases (PTPs) is a critical element in the regulation of signal transduction pathways that control processes as diverse as cell growth, proliferation, and differentiation (*1*). PTP1B is the founding member (*2*) of a family of more than 40 PTPs, including receptorlike transmembrane forms and cytosolic enzymes, that are characterized by homologous catalytic domains of ~240 amino acids (*1*). Each PTP has an 11-residue sequence motif that contains the catalytically essential Cys and Arg residues (*3*) and that is also shared by the dual-specificity phosphatases such as Cdc25 (*4*) and mitogen-activated protein (MAP) kinase phosphatase–1 (*5*). Crystallographic investigations of PTP1B (*6*) and *Yersinia* PTP (*7*) have revealed that this motif forms a phosphate binding site similar in conformation to that observed in an acid phosphatase, also described as a low molecular mass PTP (*8–10*).

PTP1B specifically dephosphorylates pTyr-containing proteins (*11*). Free pTyr is a relatively poor substrate [Michaelis constant (K_m), 5 mM] compared with pTyr peptides, suggesting that the primary determinant of specificity is a pTyr residue in the context of a peptide and that flanking residues confer additional binding affinity (*12–14*). Kinetic studies of PTP1B, *Yersinia* PTP (*12–14*), TC-PTP (*15*), and PTPβ (*16*) with diverse synthetic peptides have demonstrated sequence specificity, with K_m values ranging over three orders of magnitude, and that individual PTPs differ in their capacity to dephosphorylate a given peptide. Peptides with acidic amino acids within five residues NH_2-terminal to the pTyr site are the preferred substrates, whereas similarly positioned Arg residues reduce binding affinity (*12–17*). In contrast, Src homology 2 (SH2) domains, which recognize pTyr peptides with dissociation constants ranging over six orders of magnitude, contain binding sites both for pTyr and for residues COOH-terminal to pTyr (*18–20*).

To provide insight into the structural basis of substrate recognition by PTP1B, we determined the structures of a catalytically inactive Cys^{215} → Ser mutant form of the enzyme in complex with pTyr and the high-affinity peptides DADEpYL-NH_2 [EGFR-(988–993)] (*21*) and Ac-DEpYL-NH_2 [EGFR(990–993)] (K_m, 3.2 and ~20 μM, respectively) (*13*). These are modeled on an autophosphorylation site of the epidermal growth factor receptor (EGFR) (*22*). Details of the crystallization conditions and structure determination are provided in (*23*) and Table 1. Free pTyr and residues of the phosphopeptides bound to PTP1B were fitted unambiguously to well-defined electron density, although that for the residue at position 1 (corresponding to the P-4 site) of the hexapeptide was weak, suggesting conformational flexibility (Fig. 1). Least-squares superimposition of the PTP1B-substrate complexes showed that their conformations are essentially identical (*24*). Comparison of the PTP1B-peptide complexes with both the unliganded native (*6*) and the Cys^{215} → Ser mutant enzymes showed that the protein structures are similar, with conformational changes confined to residues at the ligand binding site (*24*). The general feature of peptide binding to PTP1B is that the pTyr side chain extends into a deep recognition pocket whose base corresponds to the phosphate binding site located on a loop connecting β12 with α4 (*6*). The orientation of the peptide is perpendicular to the parallel region of the central β sheet (Fig. 2).

Binding of either phosphopeptide or pTyr to PTP1B was accompanied by a conformational change of a surface loop consisting of residues Trp^{179} to Ser^{187} that brings Asp^{181} and Phe^{182} into the catalytic site (Fig. 3). Main-chain atoms shift by as much as 5.5 Å, with the side chains of Asp^{181} and Phe^{182} shifting by 8 and 12 Å, respectively, toward the pTyr binding site. In the unliganded structure, the side chain of Asp^{181} forms a salt bridge with the side chain of Arg^{112} (*6*). The closed conformation of the loop is stabilized by (i) hydrophobic interactions between the side chain of Phe^{182}

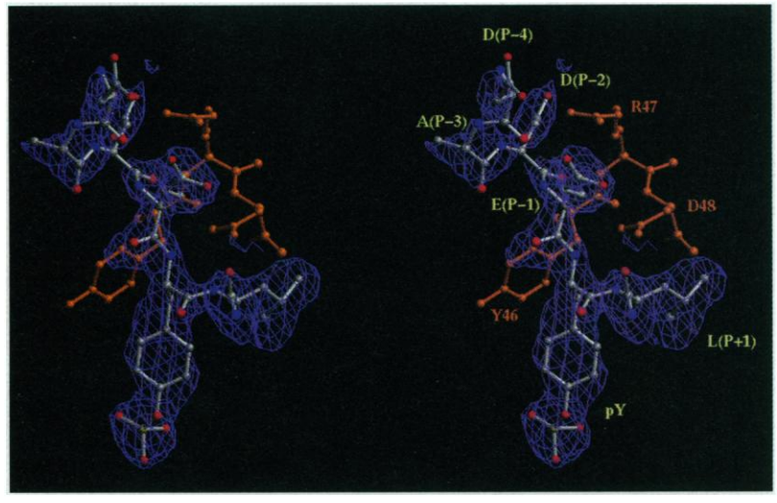

Fig. 1. Stereo view of the "omit" electron density for the hexapeptide in the hexapeptide-PTP1B complex structure. The map is contoured at 2.5σ to 2.6 Å, with the refined model of the hexapeptide (DADEpYL-NH_2) superimposed. In calculating the omit map, the peptide was excluded in both refinement and map calculation. Reference residues Tyr^{46}, Arg^{47}, and Asp^{48} are also shown colored brown. Figures were produced with SETOR (*39*) unless otherwise indicated.

Z. Jia and D. Barford, Laboratory of Molecular Biophysics, University of Oxford, Oxford OX1 3QU, UK.
A. J. Flint and N. K. Tonks, Cold Spring Harbor Laboratory, Cold Spring Harbor, NY 11724, USA.
*To whom correspondence should be addressed.

and the phenyl ring of pTyr; (ii) a hydrogen bond between a buried water molecule and the main-chain nitrogen of Phe^{182}; and (iii) a salt bridge between the side chains of Asp^{181} and Lys^{120} (Figs. 3 and 4A). A conformational change of the equivalent loop in *Yersinia* PTP is induced by tungstate binding to the catalytic site (*7*), although this change is not observed with tungstate bound to PTP1B (*6*). The side chain of Phe^{182} is approximately perpendicular to the pTyr phenyl ring and forms additional contacts with the side chains of Gln^{262} and Thr^{263}. Although Phe^{182} plays a key role in developing the catalytic site structure, it is not well conserved within the PTP family, suggesting variation in the structure of PTP catalytic sites.

Nonpolar residues, many of which are invariant within the PTP family (Figs. 2 and 4), form the recognition site for the phenyl ring of pTyr. These residues include the side chains of Ala^{217} and Ile^{219} of the PTP signature motif, Tyr^{46}, Val^{49}, Phe^{182}, and the aliphatic moiety of the side chain of Gln^{262}. The side chain of Tyr^{46} forms interactions with the main-chain atoms and the aromatic ring of pTyr. A hydrogen bond between the OH group of Tyr^{46} and the side chain of Ser^{216} stabilizes the conformation of Tyr^{46} and its interaction with the substrate. Residues Tyr^{46}, Ser^{216}, and Ala^{217} are invariant among eukaryotic PTPs, suggesting a similar mode of substrate binding. In the *Yersinia* PTP, a Phe residue is present instead of Tyr^{46}, suggesting that the mechanism of pTyr recognition may be conserved in this enzyme. An Ile residue is present at the equivalent position of Ile^{219} of PTP1B in the phosphate binding cradle of the low molecular mass PTP, which, together with the observation that other hydrophobic residues line the catalytic site cleft of the low molecular mass PTP, suggests similarities in pTyr binding with PTP1B.

The catalytic site, formed from residues Cys^{215} to Arg^{221} corresponding to the conserved PTP signature motif, is located at the base of the pTyr binding pocket. Main-chain nitrogens of Ser^{216} to Arg^{221} and the guanidinium side chain of Arg^{221} form six hydrogen bonds and two salt bridges, respectively, with the three terminal phosphate oxygens of pTyr (Fig. 4, A and C). This phosphate binding cradle is roughly planar and would favor formation of the planar trigonal transition state intermediate. The Oγ atom of Ser^{215}, situated within the center of the cradle, is 3.2 Å from the phosphorus atom of pTyr, placing Ser^{215} Oγ and the pTyr phosphorus and phenolic oxygen atoms approximately colinear and indicating that a Cys residue at position 215 would be ideally positioned for nucleophilic reaction with the substrate phosphorus. The phenolic oxygen atom of pTyr forms a network of hydrogen bonds with the side chain of Asp^{181} and, as indicated by the electron density maps, a buried water molecule (Fig. 4, A and C). A hydrogen bond between the phenolic oxygen of pTyr and Asp^{181} requires protonation of the latter residue, suggesting that Asp^{181} may function as a general acid catalyst by protonating the phenolic oxygen atom and facilitating bond cleavage. The structure also suggests that the proton from the side chain of Asp^{181} may be conducted to the substrate via the buried water molecule. Our results are consistent with the proposed role of Asp^{356} of *Yersinia* PTP (equivalent to Asp^{181} of PTP1B) as a general acid (*25*) and the observation that the side chain of Asp^{356} is within ~3.5 Å of an oxygen of tungstate bound to the catalytic site of *Yersinia* PTP (*7*). The increased pK_a (negative logarithm of the acid constant) of Asp^{181} may result from the close proximity to the phosphate of pTyr and the side chain of Glu^{115} (4.3 Å). The putative general acid Asp^{129} of the low molecular mass PTP (*8*, *9*, *26*, *27*) adopts a position similar to that of Asp^{181} of PTP1B and forms a hydrogen bond with an oxygen of a sulfate or phosphate bound to the catalytic site of the bovine enzyme (*8*, *9*).

Residues at the P−4 and P−2 through P+1 sites of the hexapeptide form interactions with the protein (Figs. 2 and 4, B and C). Although the main-chain conformation NH_2-terminal to the pTyr residue is a twisted β strand, the pTyr residue adopts a right-handed α-helical conformation. Phosphotyrosine peptides bound to SH2 domains adopt a β-strand conformation (*18*–*20*), as do the consensus residues of a peptide at the catalytic site of protein kinase A (*28*). A primary determinant of the peptide conformation at the pTyr site is the formation of two hydrogen bonds between main-chain nitrogens of pTyr and the P+1 residue with the side chain of Asp^{48}. These hydrogen bonds are important because they stabilize a helical main-chain conformation at the pTyr site of the peptide and, in part, define the peptide orientation. The Asp^{48} (or Asn) residue is highly conserved in other PTPs,

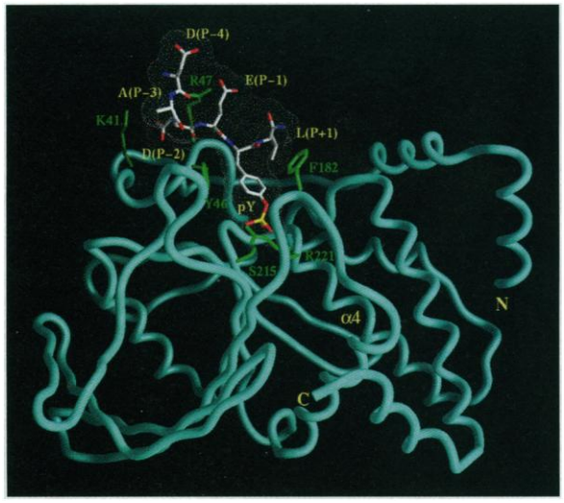

Fig. 2. Overall view of the hexapeptide-PTP1B complex structure. The side chain of pTyr extends 9 Å into the recognition pocket. The main-chain backbone of PTP1B is represented in blue. The peptide is represented as bonds with its molecular surface indicated as white dots. The side chains of K41, Y46, R47, F182, S215, and R221 of PTP1B are also indicated in green (*21*). The figure was produced with GRASP (*40*). N and C, NH_2- and COOH-termini of PTP1B, respectively. The phosphate-binding site is situated at the NH_2-terminus of α4.

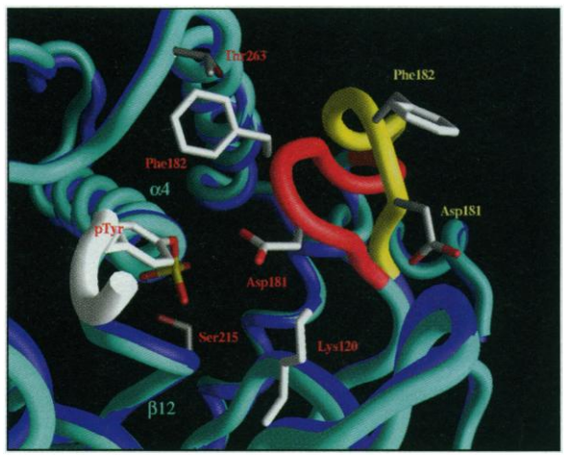

Fig. 3. Comparison of the Trp^{179} to Ser^{187} loop in unliganded native PTP1B (*6*) and the hexapeptide-PTP1B complex structures. The loop backbone (consisting of residues 179 to 187) is colored yellow and red for the uncomplexed and peptide complex forms of PTP1B, respectively. Other regions of the polypeptide chain are colored blue and cyan for the uncomplexed and peptide complex forms of PTP1B, respectively. The pTyr peptide backbone is in white. The side chains of Asp^{181} and Phe^{182} are shown for both structures with the side chains of Lys^{120}, Ser^{215}, Thr^{263}, and pTyr of the hexapeptide-PTP1B complex. The figure was produced with GRASP (*40*). The base of the catalytic site is located on the loop connecting β12 with α4.

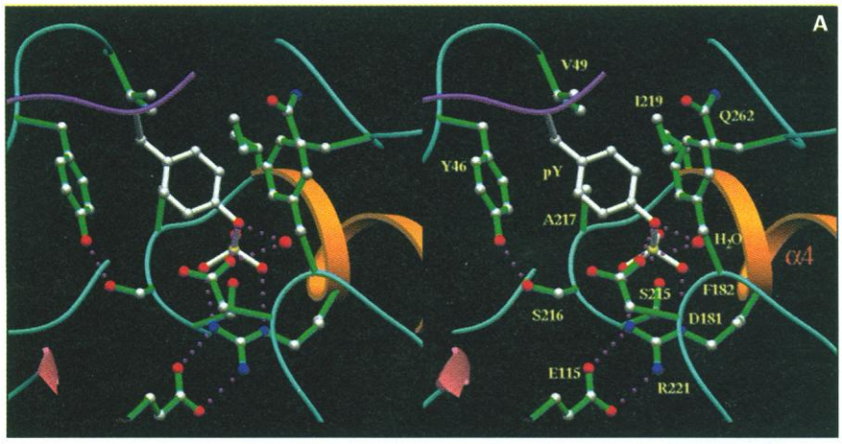

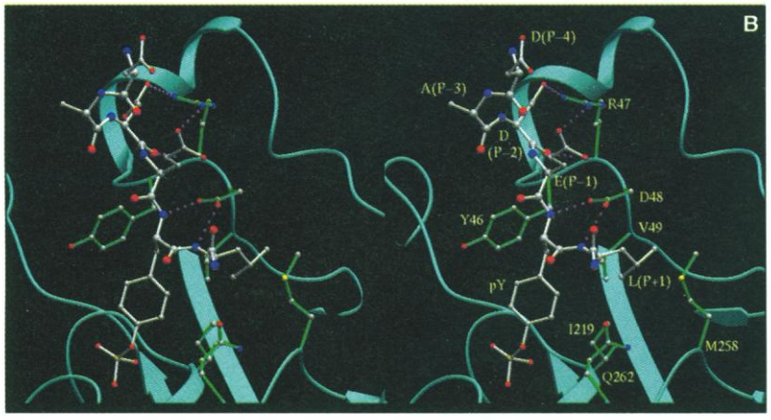

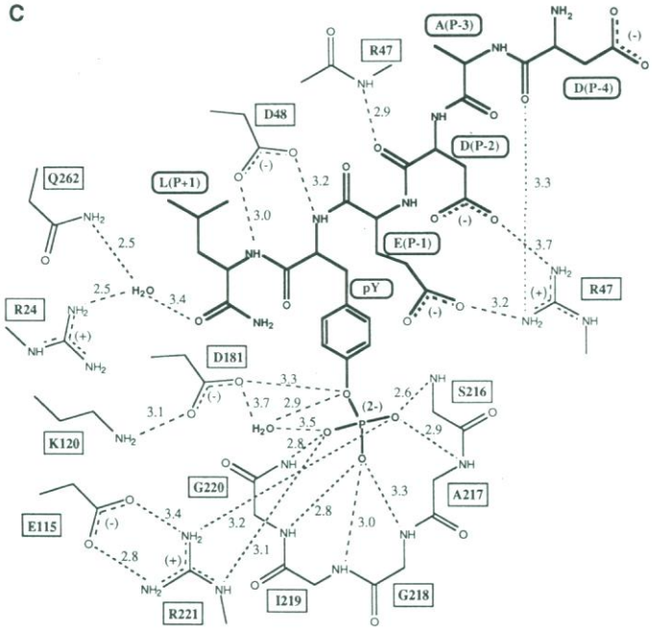

Fig. 4. Views of the pTyr binding pocket (**A**) and hexapeptide binding interactions (**B**), and schematic representation showing potential hydrogen bonding and electrostatic interactions (**C**). In (A), the hexapeptide backbone is in purple and pTyr in white. Side chains of Y46, V49, E115, D181, F182, S215, S216, A217, I219, R221, and Q262 are highlighted in green (*21*). A buried water molecule is also shown. The purple dotted lines indicate hydrogen bonds and salt bridges. The guanidinium group of Arg^{221} shifts by 2.0 Å in order to form two salt bridges with the phosphate oxygens of pTyr as a result of ligand binding. Main-chain torsion angles for Ser^{215}, or Cys^{215} of wild-type PTP1B, adopt slightly unfavorable conformations ($\phi = -133°$, $\varphi = -143°$). This deviation from more favorable conformations may play a role in positioning the side chain of Cys^{215} for nucleophilic reaction with the substrate. The hydrogen bond between the side chain of the invariant His^{214} and main-chain oxygen of Ser^{215} or Cys^{215} (not shown) may stabilize the main-chain conformation at position 215 (*6*). In (B) the peptide is shown in white and the side chains of Y46, R47, D48, V49, I219, M258, and Q262 of PTP1B are shown in green. The purple dotted lines indicate the interactions of the side chain of R47 with the side chains of E(P−1) and D(P−2) and the main-chain oxygen of D(P−4), and of the side chain of D48 with main-chain nitrogen atoms of pY and L(P+1). In (C) dashed lines represent interactions between PTP1B and the hexapeptide. A distance cutoff of 3.7 Å is used. The hexapeptide is shown in bold.

suggesting a general role in peptide recognition. A hydrogen bond is formed between the main-chain carbonyl of P−2 and the main-chain nitrogen of Arg^{47}. Peptide binding induces movement of the guanidinium group of Arg^{47} by 3.5 Å to form salt bridges with the side chains at the P−2 and P−1 positions of the peptide and a long hydrogen bond (3.2 Å) with the main-chain carbonyl at P−4 (Figs. 2 and 4, B and C). This latter hydrogen bond may explain the sixfold higher affinity of the enzyme for the hexapeptide than for the tetrapeptide (*13*). The side chain of Leu at P+1 of the peptide is located on a hydrophobic region of the protein surface and forms van der Waals contacts with the side chains of Val^{49}, Ile^{219}, and Gln^{262} and the edge of the phenyl ring of pTyr. A water-mediated hydrogen bond between the P+1 amide group and the side chain of the invariant Gln^{262} is also observed.

The interactions of Arg^{47} with acidic side chains of the peptide are consistent with kinetic data suggesting a preference for peptides with acidic amino acids NH_2-terminal to pTyr (*12–14*), which often are present in physiologically occurring pTyr proteins (*29, 30*). *Yersinia* PTP and TC-PTP, which both contain Arg at the equivalent position of Arg^{47} of PTP1B, also have a kinetic preference for peptides with acidic residues NH_2-terminal to the pTyr site (*12, 15*). PTPs with other residues at this position may show different sequence specificities. Peptides with either Asp or Glu at positions P−3, P−2, and P−1 are good substrates for PTP1B (*12, 14, 31*). The PTP1B structure shows that either acidic residue could be accommodated at the P−3, P−2, and P−1 sites and could form interactions with basic residues of the protein. For instance, the side chain of Lys^{41} is oriented toward the P−3 and P−2 sites of the peptide. With Asp at P−2, the interaction is long (4.6 Å); however, model-building studies indicate that a Glu at P−2 would interact with Lys^{41} (Fig. 2). Kinetic data [which show that additional residues NH_2-terminal to Asp(P−4) and COOH-terminal to Leu(P+1) of the $EGFR_{(988–993)}$ peptide confer essentially no increase in binding affinity (*13*)] suggest that the structure described here accounts for most of the peptide-protein interactions. The nature of

Table 1. Results of crystal structure determination of PTP1B complexes (*21*). We prepared PTP1B-pTyr crystals by soaking crystals of the inactive C215S mutant of PTP1B in crystallization buffer with 5 mM pTyr (Sigma) for 1 hour. PTP1B-peptide complex crystals were grown under similar conditions to those used for native crystals with the exception that the protein was mixed with a threefold excess of peptide (Genosys Biotechnologies) before crystallization. Crystals were incubated in crystallization buffer with the respective ligands and 25% (v/v) glycerol for 40 min before being frozen at 100 K for data collection. All data were processed with DENZO (*34*) and reduced with the CCP4 package (*33*). The pTyr-PTP1B crystals are isomorphous with native PTP1B crystals, and the coordinates of native PTP1B (*6*) [PDB code 2HNP (*35*)] were used in the initial refinement of the pTyr-PTP1B crystal form. Refinement with X-PLOR (*36*) and manual model building with program O (*37*) resulted in a structure that included an additional α helix at the COOH-terminus (residues 283 to 298) and three residues at the NH_2-terminus (residues 2 to 4). Binding of peptides to PTP1B results in a 20 Å expansion of the unit cell along *c*. The tetrapeptide-PTP1B crystal form, which is isomorphous with the hexapeptide-PTP1B crystal, was solved by molecular replacement with the pTyr-PTP1B model, excluding the pTyr ligand, and programs AMoRe (*38*).

Parameters	PTP1B complexes		
	DADEpYL-NH_2	Ac-DEpYL-NH_2	Phosphotyrosine
Crystal parameters			
Space group	$P3_121$	$P3_121$	$P3_121$
a (Å)	88.4	88.5	88.2
b (Å)	88.4	88.5	88.2
c (Å)	123.6	124.5	103.6
Z	1	1	1
Data collection and processing statistics			
Resolution* (Å)	50.0 to 2.6	50.0 to 2.9	50.0 to 2.3
Crystals (*n*)	1	1	1
Measurements (*n*)	103,993	86,391	146,758
Unique reflections (*n*)	15,101	10,478	21,436
Complete (%)	84.6	80.7	99.7
R_{sym}†	0.095	0.057	0.035
Mean $I/\sigma I$	12.7	14.4	17.9
X-ray source‡	SRS PX9.5	SRS PX7.2	BNL X12C
λ (Å)§	0.89	1.49	1.07
Refinement statistics			
Resolution (Å)	6.0 to 2.6	6.0 to 2.9	6.0 to 2.3
Reflections (*n*) ($F > 2\sigma F$) (% complete)	14,754 (82.6)	9,025 (79.1)	19,460 (97.8)
Protein and ligand atoms	2,482	2,471	2,444
Water molecules (*n*)	71	0	259
R factor‖	0.199	0.194	0.172
rmsd bond lengths (Å)‖	0.018	0.021	0.017
rmsd bond angles (degrees)¶	2.10	2.18	1.92

*Practical diffraction limits of the crystal. †$R_{sym} = \Sigma_h\Sigma_i|I_i(h) - I_i(h)|/\Sigma_h\Sigma_i I_i(h)$, where $I_i(h)$ and $I(h)$ are the *i*th and mean measurements of the intensity of reflection *h*. ‡SRS PX7.2, Synchrotron Radiation Source, Daresbury Laboratory, United Kingdom, station PX 7.2 equipped with an 18-cm MAR Research Image Plate. SRS PX9.5, Synchrotron Radiation Source, station PX 9.5 equipped with a 30-cm MAR Research Image Plate. BNL X12C, Brookhaven National Laboratory, National Synchrotron Light Source, Upton, New York, station X12C equipped with a 30-cm MAR Research Image Plate. §λ, wavelength. ‖*R* factor $= \Sigma_h||F_o| - |F_c||/\Sigma_h|F_o|$, where F_o and F_c are the observed and calculated structure factor amplitudes of reflection *h*. ¶rmsd, Root-mean-square deviation from ideality.

these interactions is also consistent with kinetic data that show that phosphopeptides with less than four residues display significantly increased K_m values (*13*).

The structure of PTP1B complexed with a peptide derived from a physiologically relevant autophosphorylation site of the EGFR reveals the molecular mechanisms of substrate recognition. The recognition pocket for pTyr is the dominant feature of the peptide binding site (Figs. 2 and 4). Phosphotyrosine contributes ~53% of the peptide solvent-accessible surface area (*32*) buried as a result of hexapeptide binding. Specificity for pTyr peptides is achieved through numerous mechanisms, one of which is the depth of the amphipathic pTyr binding pocket—defined by Arg^{221} at its base and Asp^{48} at the rim and which exactly matches the length of a pTyr residue (~9 Å) (Fig. 2). The side chains of pSer and pThr are too short to reach to the catalytic residues at the base of the cleft. Selectivity for pTyr residues on the basis of length has been proposed to explain the specificity of SH2 domains for pTyr-containing peptides (*18–20*), although the nonpolar nature of the phenyl group–protein interactions observed in the PTP1B-substrate complex contrasts with the amino-aromatic interactions apparent between the phenyl group of the pTyr residue and the side chains of Arg and Lys at the pTyr binding site of the SH2 domains of Src (*18*) and Lck (*19*). Other determinants of specificity include (i) the presence of nonpolar side chains lining the cleft that form hydrophobic interactions with the phenyl group of the pTyr residue and (ii) the formation of hydrogen bonds between peptide main-chain atoms and the protein. The interactions between the peptide side chains and basic residues on the protein surface confer sequence specificity; however, the relatively open structure of the peptide binding site is consistent with the ability of PTP1B to dephosphorylate a variety of pTyr substrates. PTPs constitute a diverse family of signal-transducing enzymes. The structural data reported here should provide a basis for understanding substrate recognition by other PTPs.

REFERENCES AND NOTES

1. H. Charbonneau and N. K. Tonks, *Annu. Rev. Cell Biol.* **8**, 463 (1992); K. M. Walton and J. E. Dixon, *Annu. Rev. Biochem.* **62**, 101 (1993); N. K. Tonks, Ed., *Semin. Cell Biol.* **4**, 373 (1993).
2. N. K. Tonks, C. D. Diltz, E. H. Fischer, *J. Biol. Chem.* **263**, 6722 (1988).
3. M. Streuli, N. K. Krueger, T. Thai, M. Tang, H. Siato, *EMBO J.* **9**, 2399 (1990); K. L. Guan and J. E. Dixon, *J. Biol. Chem.* **266**, 17026 (1991); D. A. Pot, T. A. Woodford, E. Remboutsika, R. S. Haun, J. E. Dixon, *ibid.*, p. 19688; H. Cho *et al.*, *J. Am. Chem. Soc.* **114**, 7296 (1992).
4. J. B. A. Millar and P. Russell, *Cell* **68**, 407 (1992).
5. H. Sun, C. H. Charles, L. F. Lau, N. K. Tonks, *ibid.* **75**, 487 (1993); D. R. Alessi, C. Symthe, S. M. Keyes, *Oncogene* **8**, 2015 (1993).
6. D. Barford, A. J. Flint, N. K. Tonks, *Science* **263**, 1397 (1994).
7. J. A. Stuckey *et al.*, *Nature* **370**, 571 (1994).
8. X.-D. Su, N. Taddei, M. Stefani, G. Ramponi, P. Nordlund, *ibid.*, p. 575.
9. M. Zhang, R. L. Van Etten, C. V. Stauffacher, *Biochemistry* **33**, 11097 (1994).
10. T. M. Logan *et al.*, *ibid.*, p. 11087.
11. N. K. Tonks, C. D. Diltz, E. H. Fischer, *J. Biol. Chem.* **263**, 6731 (1988).
12. Z.-Y. Zhang *et al.*, *Proc. Natl. Acad. Sci. U.S.A.* **90**, 4446 (1993).
13. Z.-Y. Zhang, D. Maclean, D. J. McNamara, T. K. Sawyer, J. E. Dixon, *Biochemistry* **33**, 2285 (1994).
14. K. L. Hippen *et al.*, *ibid.* **32**, 12405 (1993).
15. M. Ruzzene *et al.*, *Eur. J. Biochem.* **211**, 289 (1993).
16. H. Cho *et al.*, *Protein Sci.* **2**, 977 (1993).
17. L. A. Pinna and A. Donella-Deana, *Biochem. Biophys. Acta* **1222**, 415 (1994).
18. G. Waksman *et al.*, *Nature* **358**, 646 (1992); G. Waksman, S. E. Shoelson, N. Pant, D. Cowburn, J. Kuriyan, *Cell* **72**, 779 (1992).
19. M. J. Eck, S. E. Shoelson, S. C. Harrison, *Nature* **362**, 87 (1993).
20. C.-H. Lee *et al.*, *Structure* **2**, 423 (1994).
21. Abbreviations for the amino acid residues are: A, Ala; C, Cys; D, Asp; E, Glu; F, Phe; G, Gly; H, His; I, Ile; K, Lys; L, Leu; M, Met; N, Asn; P, Pro; Q, Gln; R, Arg; S, Ser; T, Thr; V, Val; W, Trp; and Y, Tyr. Ac, acetal group; pY, phosphotyrosine.
22. G. M. Walton, W. S. Chen, M. G. Rosenfeld, G. N. Gill, *J. Biol. Chem.* **265**, 1750 (1990).
23. The C215S mutation was introduced into the full-length complementary DNA by a polymerase chain reaction–based method [A. J. Flint, M. F. B. G. Gebbink, B. R. J. Franza, D. E. Hill, N. K. Tonks, *EMBO J.* **12**, 1937 (1993)], and the sequence encoding residues 1 to 321 was cloned into a T7 expression vector. The protein was expressed, purified, and crystallized as described [D. Barford, J. C. Keller, A. J. Flint, N. K. Tonks, *J. Mol. Biol.* **239**, 726 (1994)].
24. Least-squares superimpositions were performed with CCP4 programs (*33*). After superimposition, the root-mean-square (rms) deviation of main-chain atoms between the PTP1B-hexapeptide complex and

the PTP1B-tetrapeptide complex is 0.26 Å, and those between the PTP1B-pTyr complex and the PTP1B-hexapeptide and PTP1B-tetrapeptide complexes are 0.38 and 0.40 Å, respectively. Equivalent atoms of the hexapeptide and tetrapeptide superimpose within an rms deviation of 0.54 Å. The side chain of free pTyr superimposes exactly with the side chain of pTyr within the peptides. The rotomer conformation of free pTyr differs from that of a pTyr residue in a peptide because the Cα–Cβ bond is rotated 120° to avoid close contact of its COOH group with the side chain of Asp^{48}. Excluding residues 179 to 187, the rms deviation of main-chain atoms between the PTP1B-hexapeptide complex and unliganded PTP1B is 0.45 Å. The structures of unliganded wild-type and C215S PTP1B are essentially identical (Z. Jia and D. Barford, unpublished data).
25. Z.-Y. Zhang, Y. Wang, J. E. Dixon, *Proc. Natl. Acad. Sci. U.S.A.* **91**, 1624 (1994).
26. N. Taddei *et al.*, *FEBS Lett.* **350**, 328 (1994).
27. Z. Zhang, E. Harms, R. L. Van Etten, *J. Biol. Chem.* **269**, 25947 (1994).
28. D. E. Knighton *et al.*, *Science* **253**, 414 (1991); E. A. Madhusudan *et al.*, *Protein Sci.* **3**, 176 (1994).
29. R. B. Pearson and B. E. Kemp, *Methods Enzymol.* **200**, 62 (1991).
30. Z. Songyang *et al.*, *Nature* **373**, 536 (1995).
31. C. J. Pallen, D. S. Y. Lai, H. P. Chia, I. Boulet, P. H. Tong, *Biochem. J.* **276**, 315 (1991).
32. The solvent-accessible surface was calculated with the program DSSP [W. Kabsch and C. Sander, *Biopolymers* **22**, 2577 (1983)].
33. Collaborative Computational Project, Number 4, *Acta Crystallogr.* **D50**, 760 (1994).
34. Z. Otwinowski, in *Data Collection and Processing*, L. Sawyer, N. Issacs, S. Bailey, Eds. (SERC Daresbury Laboratory, Warrington, UK, 1993), p. 56.
35. F. C. Bernstein *et al.*, *J. Mol. Biol.* **112**, 535 (1977).
36. A. T. Brünger, *X-PLOR, Version 3.1* (Yale Univ. Press, New Haven, CT, 1993).
37. T. A. Jones, J. Y. Zhou, S. W. Cowan, M. Kjeldgaard, *Acta Crystallogr.* **A47**, 110 (1991).
38. J. Navaza, *ibid.* **A50**, 157 (1994).
39. S. V. Evans, *J. Mol. Graphics* **11**, 134 (1993).
40. A. Nicholls, R. Bharadwaj, B. Honig, *Biophys. J.* **64**, 166 (1991).
41. Supported by Wellcome Trust grant 042552/Z/94/Z (D.B.), Natural Sciences and Engineering Research Council of Canada (Z.J.), NIH grant CA53840 (N.K.T.), a Pew Scholar Award in the Biomedical Sciences (N.K.T.), and a Cancer Research Institute and F. M. Kirby Foundation fellowship (A.J.F.). We thank the staff at the Synchrotron Radiation Source, Daresbury, U.K.; R. M. Sweet at the National Synchrotron Light Source at Brookhaven National Laboratory, Upton, NY, for assistance with data collection; and L. N. Johnson for support and comments on the manuscript. The atomic coordinates have been submitted to the Brookhaven protein database.

6 February 1995; accepted 19 April 1995

Crystal Structure of *Pseudomonas mevalonii* HMG-CoA Reductase at 3.0 Angstrom Resolution

C. Martin Lawrence,* Victor W. Rodwell, Cynthia V. Stauffacher†

The rate-limiting step in cholesterol biosynthesis in mammals is catalyzed by 3-hydroxy-3-methylglutaryl–coenzyme A (HMG-CoA) reductase, a four-electron oxidoreductase that converts HMG-CoA to mevalonate. The crystal structure of HMG-CoA reductase from *Pseudomonas mevalonii* was determined at 3.0 angstrom resolution by multiple isomorphous replacement. The structure reveals a tightly bound dimer that brings together at the subunit interface the conserved residues implicated in substrate binding and catalysis. These dimers are packed about a threefold crystallographic axis, forming a hexamer with 23 point group symmetry. Difference Fourier studies reveal the binding sites for the substrates HMG-CoA and reduced or oxidized nicotinamide adenine dinucleotide [NAD(H)] and demonstrate that the active sites are at the dimer interfaces. The HMG-CoA is bound by a domain with an unusual fold, consisting of a central α helix surrounded by a triangular set of walls of β sheets and α helices. The NAD(H) is bound by a domain characterized by an antiparallel β structure that defines a class of dinucleotide-binding domains.

The biosynthesis of cholesterol is regulated at the level of the enzyme HMG-CoA reductase, which catalyzes the interconversion of HMG-CoA and mevalonate. This reaction is the first committed step in the pathway of isoprenoid biosynthesis. In mammals, >90% of the bulk carbon flow along this pathway is used in the production of cholesterol. Although cholesterol is an essential component of mammalian cell membranes, its deposition in atherosclerotic plaques restricts blood flow, an important factor in heart disease and death by stroke or heart attack. The abundance of mammalian HMG-CoA reductase is normally controlled through the regulation of transcription (*1*), translation (*2*), and enzyme degradation (*3*), whereas the activity of the enzyme is inhibited by phosphorylation (*4*). Inhibition of HMG-CoA reductase by drugs such as lovastatin lowers intracellular cholesterol concentrations (*5*) and increases both low density lipoprotein (LDL) receptor number and absorption of cholesterol circulating as LDL (*6*).

The reaction catalyzed by eukaryotic HMG-CoA reductase is a four-electron NADP(H)-dependent oxidoreduction that requires two molecules of NADPH to reduce HMG-CoA to mevalonate and CoA. The reaction is analogous to the two successive reactions of an aldehyde dehydrogenase and an alcohol dehydrogenase, but is accomplished by a single enzyme. Comparatively little is known of the structural requirements for catalysis by HMG-CoA reductase. Direct participation of cysteines in catalysis, suggested by sensitivity to sulfhydryl reagents (*7–10*), was disproved by elimination of cysteines by site-directed mutagenesis (*11*). Glutamate and histidine residues essential for catalysis have, however, been identified (*11–13*). Sequence analysis of >20 HMG-CoA reductases from yeast to mammals indicates a COOH-terminal catalytic domain of ~50 kD and a hydrophobic NH_2-terminal membrane-attachment domain of variable length (*14*). Mammalian HMG-CoA reductase is thought to be active as a homodimer with a monomer molecular size of 70 to 100 kD (*15*).

We have now determined the crystal structure of *Pseudomonas mevalonii* HMG-CoA reductase, a soluble protein of 45-kD subunits. Although functionally analogous to the catalytic domain of the larger mammalian enzymes, the *Pseudomonas* enzyme lacks an NH_2-terminal membrane anchor (*7, 16*). *Pseudomonas* HMG-CoA reductase, which functions as a catabolic enzyme, is induced by mevalonate, which it converts into HMG-CoA with NAD^+ as an oxidant (*7, 9, 17, 18*). Sequence identity between the *Pseudomonas* enzyme and the COOH-terminal catalytic domain of mammalian HMG-CoA reductase is limited (20%), but key residues implicated in substrate recognition and catalysis are conserved (*12, 13*).

Recombinant *P. mevalonii* HMG-CoA reductase was overexpressed in *Escherichia coli* and purified to homogeneity as previously described (*16*). Crystals were grown in the cubic space group $I4_132$ with $a = 229.4$ Å and two monomers per asymmetric unit (*19*). The structure solution (Table 1) was based on an initial multiple isomorphous replacement (MIR) map calculated from four heavy-atom derivatives. The MIR phases were refined with solvent flattening and averaging over the twofold noncrystallographic symmetry, beginning at 5.0 Å and gradually extending to 3.0 Å. The final phase-refined 3.0 Å map showed continuous main chain density from the NH_2-terminus to residue 378; the last 50 residues of the molecule are disordered in the crystal. The sequence fit to the map was confirmed from the positions of the unique 24 methionines seen in difference Fourier density based on selenomethionine-substituted HMG-CoA reductase (Fig. 1). The current model has been refined with TNT (*20*) at 3.0 Å to give a crystallographic *R* factor of 18.9% and an

C. M. Lawrence and C. V. Stauffacher, Department of Biological Sciences, Purdue University, West Lafayette, IN 47907, USA.
V. W. Rodwell, Department of Biochemistry, Purdue University, West Lafayette, IN 47907, USA.

*Present address: Howard Hughes Medical Institute and Laboratory of Molecular Medicine, Childrens Hospital, Boston, MA 02115, USA.
†To whom correspondence should be addressed.